J Physiol 596.18 (2018) pp 4537–4548

The Journal of Physiology

Multisensory activation of ventral cochlear nucleus D-stellate cells modulates dorsal cochlear nucleus principal cell spatial coding

Calvin Wu and Susan E. Shore

Kresge Hearing Research Institute, Department of Otolaryngology, University of Michigan, Ann Arbor, MI 48109, USA

Edited by: Ian Forsythe & Andrew King

Key points

- Dorsal cochlear nucleus fusiform cells receive spectrally relevant auditory input for sound localization.
- Fusiform cells integrate auditory with other multisensory inputs.
- Here we elucidate how somatosensory and vestibular stimulation modify the fusiform cell spatial code through activation of an inhibitory interneuron: the ventral cochlear nucleus D-stellate cell.
- These results suggests that multisensory cues interact early in an ascending sensory pathway to serve an essential function.

Abstract In the cochlear nucleus (CN), the first central site for coding sound location, numerous multisensory projections and their modulatory effects have been reported. However, multisensory influences on sound location processing in the CN remain unknown. The principal output neurons of the dorsal CN, fusiform cells, encode spatial information through frequency-selective responses to direction-dependent spectral features. Here, single-unit recordings from the guinea pig CN revealed transient alterations by somatosensory and vestibular stimulation in fusiform cell spatial coding. Changes in fusiform cell spectral sensitivity correlated with multisensory modulation of ventral CN D-stellate cell responses, which provide direct, wideband inhibition to fusiform cells. These results suggest that multisensory inputs contribute to spatial coding in DCN fusiform cells via an inhibitory interneuron, the D-stellate cell. This early multisensory integration circuit likely confers important consequences on perceptual organization downstream.

(Resubmitted 27 June 2018; accepted after revision 2 August 2018; first published online 3 August 2018)
Corresponding author Susan E. Shore Ph.D: 1150 W. Medical Center Dr., Ann Arbor, Michigan 48109 (734) 647–2116. Email: sushore@umich.edu

Calvin Wu received his PhD in biology from University of North Texas, where he studied cellular and network physiology in cultured cortical neurons. He is currently a postdoctoral fellow at the Kresge Hearing Research Institute, University of Michigan under the mentorship of S.E.S. His current research focuses on multisensory integration and plasticity in the auditory brainstem and their roles in auditory processing deficits or tinnitus.

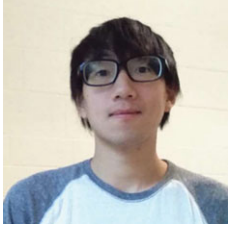

DOI: 10.1113/JP276280

Introduction

Sound localization is fundamental for survival. To ensure accurate communication and danger avoidance, neural computations of sound location utilize environmental multisensory cues (Keating & King, 2015). In mammals, many brain regions such as the superior colliculus and sensory association cortices integrate visual, somatosensory and vestibular information to create coherent auditory spatial representations (Rees, 1996; Stein *et al.* 2014). However, multisensory interactions begin much earlier in the central auditory pathway, as somatosensory and vestibular inputs modulate neural activity in the dorsal cochlear nucleus (DCN) (Kanold *et al.* 2011; Koehler *et al.* 2011; Koehler & Shore, 2013; Wigderson *et al.* 2016), a second-order station for coding sound location (May, 2000; Young & Davis, 2002). But how multisensory information functionally influences brainstem sound localization processing has not been elucidated.

Monaural cues for sound-source location are derived from direction-dependent head and pinna filtering (Blauert, 1983). Spectral 'notches' and 'edges' in the resulting acoustic signal respectively inhibit and excite principal output neurons of DCN fusiform cells (Nelken & Young, 1994; Reiss & Young, 2005). Sound-spectral features are translated into fusiform cell spike-rate coding through feed-forward, wide-band inhibition from D-stellate cells in ventral cochlear nucleus (VCN), and narrow-band inhibition from vertical cells in DCN (Nelken & Young, 1994; Rhode, 1999; Arnott *et al.* 2004; Reiss & Young, 2005; Lomakin & Davis, 2008). In addition, multisensory information from vestibular nerve and nucleus and somatosensory systems (e.g. cuneate and spinal trigeminal nuclei) is delivered to fusiform cell apical dendrites through granule cell axo-dendritic synapses (Kanold & Young, 2001; Ryugo *et al.* 2003). The multisensory projections (Burian & Gstoettner, 1988; Young *et al.* 1995; Shore & Moore, 1998) putatively 'inform' fusiform cells of head or pinna movements during sound-spectral changes. Here, we characterized fusiform cell responses to sound-spectral changes in the presence of somatosensory or vestibular activation. We found that somatosensory and vestibular stimulation both transiently altered fusiform cell response sensitivity to spectral features through modulation of D-stellate cell inhibition. The multisensory D-stellate–fusiform cell complex constitutes a novel pathway for multisensory interaction in the CN. The results suggest that at an early stage of auditory processing, multisensory integration in this unique circuit plays a crucial role in shaping perceptually relevant sound context.

Methods

Surgical preparation

Pigmented guinea pigs of both sexes ($n = 17$; 6 male, 11 female) were used. The study followed National Institutes of Health guidelines (No. 80-23) and was approved by the Institutional Animal Care and Use Committee at the University of Michigan. Ketamine (Hospira Inc., Lake Forrest, IL, USA) and xylazine (Akorn Inc., Lake Forrest, IL, USA) were used as anesthetics (initially at 50 and 5 mg kg^{-1}, respectively, then at 10 and 1 mg kg^{-1} hourly supplements, respectively). Atropine (0.05 mg kg^{-1}) was administered during the initial surgery. Local incision points were treated with lidocaine (2% w/v). Animals were fixed in a stereotaxic frame using a bite bar and hollow ear bars (Kopf) inserted into the ear canals. The core temperature was maintained at 38 ± 0.5°C using a heating pad and a rectal thermocoupler. Prior to surgery, normal hearing thresholds (10–30 dB sound pressure level (SPL)) were established with auditory brainstem responses. A left craniotomy (3 × 3 mm^2 centred at 4 mm caudal of the ear bar and 3 mm lateral of the midline) was performed for access to CN. A 16-, 32- or 64-channel silicon recording electrode (NeuroNexus, Ann Arbor, MI, USA) was inserted into the cerebellum at a 35° angle and lowered to 5.5–7 mm below the surface to span DCN and VCN enabling simultaneous recordings from fusiform and D-stellate cells. After completion of neural recordings, animals were euthanized by I.P. injection of sodium pentobarbital (Med-Pharmex Inc., Pomona, CA, USA).

Sensory stimulation

Acoustic signals were generated using OpenEx and an RX8 DSP (Tucker-Davis Technologies (TDT), Alachua, FL, USA) with a sampling rate of 100 kHz. Tone (0.2–32 kHz) and noise bursts of 10 or 50 ms duration, gated with a cosine window of 2 ms rise/fall time, were presented through a calibrated, closed-system earphone (Kopf) to the left ear (10–1000 repetitions). To simulate direction-dependent spectral features, notch-noise was constructed in MATLAB (The MathWorks Inc., Natick, MA, USA; fdatool) by applying band-reject finite-impulse response digital filters (30 dB attenuation, order = 128) to broadband noise. Upper and lower cut-off frequencies were manually selected. Somatosensory activation by dorsal column stimulation was achieved by placing electrode pads (0.375 inch Ag/AgCl, Rhythmlink, Columbia, SC, USA) on shaved neck skin overlying the ipsilateral cervical spine, C2 region (stimulating electrode: 1–2 cm lateral of midline; ground electrode: 1 cm caudal–medial of the stimulating electrode). Stimuli

consisted of three biphasic (100 μs/phase) current pulses at 1000 Hz, presented at 5 Hz for 60 s (either preceding auditory stimulation onset or following auditory stimulation offset by 10 ms). The current amplitude was set to the highest level that did not elicit movement artifact (2–4 mA). This stimulation paradigm has previously been shown to activate the fusiform cell circuit (Wu *et al.* 2015). Vestibular stimulation (linear acceleration) was achieved with a custom-built free-rotating stereotaxic platform, producing a forward pitch tilt of 20°. Notched-noise was presented during the constant tilt.

Single-unit electrophysiology and cell identification

Voltages from each recording site were amplified by a PZ2 preamplifier (TDT) and bandpass filtered (0.3–3 kHz). Spikes were detected online with automatic thresholding (2.5 SD above background noise). After removal of electrical-stimulation artifacts, digitalized waveforms were sorted offline into single units by clustering the waveform principal components using a customized algorithm in MATLAB. Putative fusiform cells were identified by (1) histological identification of the electrode-site location in the fusiform cell layer, and (2) pauser build-up or build-up temporal responses (Rhode *et al.* 1983) and classification into I/III, III, or IV-T receptive field that reflects the degree of inhibition in their receptive fields (Stabler *et al.* 1996). Type II receptive fields from putative vertical cells were rarely encountered in this study. D-stellate cells in VCN were histologically identified by electrode locations on more distal recording sites, broad tuning and onset-chopping or onset-gradual (On-C/On-G) temporal patterns (Arnott *et al.* 2004). Cross-unit interactions between D-stellate and fusiform cell spontaneous activity (recorded for 10 min) was examined using unbiased cross-correlation of spike trains: $R(N_A \times N_B)^{-0.5}$, where cross-correlation function R (bin: 0.1 ms) was normalized by the geometric mean of spike count N in spike trains A and B. Spike train stationarity was established ($P < 0.001$, augmented Dickey–Fuller test) prior to cross-correlation analyses.

Tract tracing and histology

Tracing experiments were performed to identify somatosensory projections to VCN D-stellate cells as previously described (Heeringa *et al.* 2018). FluoroRuby (5%; 0.5 μl; Thermo Fisher Scientific, Waltham, MA, USA) and FluroEmerald (10%; 0.5 μl, Thermo Fisher Scientific, Waltham, MA, USA) were pressure-injected (0.1 μl min^{-1}) into the contralateral VCN for retrograde tracing (35° angle, 3.5 mm lateral to midline, 8 mm from the dural surface) to identify D-stellate cells that comprise part of the CN-commissural pathway (Cant & Gaston, 1982; Shore *et al.* 1992; Schofield & Cant, 1996) and ipsilateral cuneate nucleus for anterograde tracing (2 mm lateral to midline, 8.5 mm from the dural surface). Animals were allowed to recover for 5 days before transcardial perfusion (100 mL 1× PBS, 400 mL 4% paraformaldehyde; after euthanasia). The brains were extracted, post-fixed for 2 h, immersed in 30% sucrose solution for 2 days, frozen and cryosectioned at 30 μm in the coronal plane (Leica, CM3050S). Coverslipped brain sections were examined under confocal epifluorescence (PMT; Leica, SP5-x). Retrogradely labelled somata of the CN-commissural pathway in the ipsilateral VCN were identified by size, with long diameters >25 μm identified as D-stellate cells (Arnott *et al.* 2004; Doucet *et al.* 2009).

Statistics

Statistical significance for numerical data was tested using Student's t test, Kolmogorov–Smirnov test, and one-way or two-way repeated-measure analysis of variance (ANOVA). The Tukey–Kramer correction was used for all *post hoc* tests. Distributions of categorical data were tested using Pearson's χ^2 test. Hartigan's dip test was used for unimodality of sample distributions. The augmented Dickey–Fuller test was used to establish spike train stationarity. Significance was established at $\alpha = 0.05$. Power analysis was performed a priori to estimate (1) the number of stimulus repetitions to achieve invariant spike rate across trials, and (2) the number of units required to establish statistical difference of >±5% in population responses.

Results

Fusiform-cell spectral-notch sensitivity is determined by inhibition strength

To examine spectral-notch coding, we first presented spectral-notch stimuli with varying widths centred at the fusiform cell's best frequency (BF; Fig. 1*A*), which mimics the mid-frequency notches of 15–35 dB depth in the guinea pig head-related transfer function (Palmer & King, 1985; Sterbing *et al.* 2003; Greene *et al.* 2014). Spectral notches of gradually increasing widths progressively reduced the fusiform cell's firing rate to below its spontaneous rate (Fig. 1*B*). This type of inhibitory response, consistent with previous reports in cats and gerbils (Nelken & Young, 1994; Parsons *et al.* 2001), was then quantified by measuring the notch width required to reduce fusiform cell firing to its spontaneous rate (Fig. 1*B*). Inhibition width (*I*-width) thus indicates fusiform cell response sensitivity to spectral notches. Across the fusiform cell population, we found two distinct groups (non-unimodal, Hartigan's dip test: $D = 0.04$, $P = 0.005$; Fig. 1*C*): some units were sharply tuned (ST) to notches of narrow widths, with low *I*-width values indicating high sensitivity, while other units were widely tuned (WT), with high *I*-width values indicating

low sensitivity. Distribution of ST and WT responses were uniform across unit BFs (2–18 kHz; Kolmogorov–Smirnov test, $D = 0.15$, $P = 0.29$; Fig. 1*C*). The 0.9 octave cut-off between the two populations corresponded well with the largest observed bandwidth in the guinea pig head-related transfer function (Greene *et al.* 2014), suggesting that ST units may be the primary responder to monaural sound localization cues. Further examination of fusiform cell types revealed that ST responses occurred exclusively in type II (putative vertical cells), III and IV-T units, while WT responses occurred predominantly in type I/III units (Fig. 1*D*; Table 1). Thus, two populations of fusiform cells with different spectral-notch sensitivities are distinguished by the amount of inhibition present in their response areas.

Table 1. Pearson's χ^2 results comparing ratios of ST and WT response for each fusiform cell type (df = 1)

χ^2	IV-T	III	I/III	II
II	2.90	2.79	12.14**	—
I/III	8.02*	18.66***	—	—
III	1.18	—	—	—

χ^2 values are shown for comparisons between column and row. ST:WT ratio for type II, III and type IV-T units are significantly different from type I/III. $^*P < 0.05$, $^{**}P < 0.01$, $^{***}P < 0.001$.

Fusiform cells in guinea pig are insensitive to rising spectral edges

While fusiform cell inhibition by spectral notches is a putative neural mechanism for sound-location coding, some fusiform cells in cats are *excited* by rising spectral edges, when aligned with the unit BFs (Reiss & Young, 2005). To assess whether guinea-pig fusiform cells also encode spectral cues via edge excitation, we presented constant-width (1 octave) spectral notches at different rising edge frequencies (0.5 octave below, aligned at BF, 0.5 or 1 octave above the unit BF; Fig. 2*A*). In contrast to cat, few units in guinea pig showed edge excitation (rising-edge-sensitive; RE+; Fig. 2*B*), while others were edge-insensitive (RE−; Fig. 2*C*). Spectral-edge sensitivity was then quantified by the edge ratio, with values >1 indicating rising-edge excitation (Fig. 2*D*). Across the fusiform cell population (Fig. 2*D*), the edge-ratio distribution was unimodal (Hartigan's dip test: $D = 0.03$, $P = 0.81$; in contrast to Fig. 1*C*), and only a small proportion of type IV-T and type III fusiform cells showed RE+ responses ($\chi^2(2) = 6.3$, $P = 0.042$; Fig. 2*E*). This

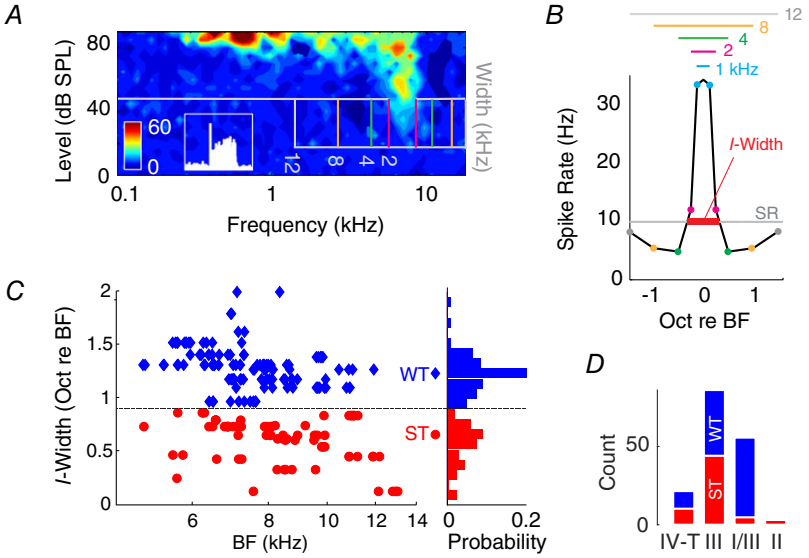

Figure 1. Spectral-notch sensitivity of fusiform cells is correlated with inhibition
A, receptive field of a representative type III fusiform cell. Spectral notches (30 dB attenuation; 30 dB SL) with different bandwidths (cut-off frequencies marked by vertical lines) are centred near the unit's BF. Inset: peri-stimulus time histogram of the same neuron in response to 20 dB sensation level (SL) tone at BF, showing a pause–build-up response (scale: 60 spikes s^{-1} × 0.1 s). *B*, fusiform cell firing rate is plotted as a function of lower and upper notch-cut-off frequencies. Notches of different bandwidths (also shown by vertical lines in *A*) and corresponding lower and upper cut-off frequencies are indicated by coloured horizontal lines and circles. The 0-octave centre point represents the unit's response to broad-band noise (BBN; 500 repetitions for each notch stimulus). Sensitivity to notch inhibition is quantified by *I*-width, which indicates the minimum notch width required to reduce the unit's firing spontaneous rate (SR). *C*, *I*-width distribution of the fusiform cell population ($n = 206$) as a function of unit best frequency (BF) and probability (bin: 0.1 octaves). Units with *I*-widths <0.9 octave (dip in distribution) are classified as sharp-tuning (ST), and those >0.9 octaves are classified as wide-tuning (WT). *D*, distribution of ST and WT responses across fusiform cell types (see Table 1 for statistics).

suggests that notch inhibition, rather than edge excitation, is used as the primary mechanism of spectral-feature detection in the guinea pig DCN.

Somatosensory and vestibular stimulation alters spectral-notch detection sensitivity in fusiform cells

For multisensory inputs to provide fusiform cells with relevant information regarding head (or pinna in cats) movement, sensory-stimulus timing must follow a specific behavioural sequence (e.g. whether head/pinna movement precedes or follows sound detection). Thus, we tested two timing paradigms: auditory preceding somatosensory (AP) or somatosensory preceding auditory (SP) stimulation (Fig. 3*A*). In a representative unit (Fig. 3*B*), *I*-width decreased from the naïve condition during AP stimulation to indicate a sensitized response. Across the population of fusiform cells, somatosensory effects on notch-detection sensitivity were observed only in ST units, and were order-sensitive (two-sample Kolmogorov–Smirnov test, $D = 0.57$, $P = 0.0006$ for ST *vs.* WT; $D = 0.83$, $P = 0.0087$ for AP *vs.* SP): AP stimuli increased notch-detection sensitivity (two-sample t test, $t(52) = -5.08$, $P = 5.1 \times 10^{-6}$), and SP stimuli decreased notch-detection sensitivity ($t(52) = 4.4$, $P = 5.3 \times 10^{-5}$; Fig. 3*C*). These modulations were transient, as *I*-widths recovered immediately after cessation of somatosensory stimulation (one-way repeated-measure ANOVA, $F(2) = 7.4$, $P = 0.006$ for AP; $F(2) = 9.6$, $P = 0.0008$ for SP; Fig. 3*D*), suggesting that somatosensory inputs can dynamically sensitize or reduce spectral notch response of fusiform cells depending on the timing of the sensory signals.

In addition to the somatosensory input, vestibular projection to the CN has also been well documented (Burian & Gstoettner, 1988; Kevetter & Perachio, 1989; Bukowska, 2002). Previous studies have also revealed a vestibular contribution in human sound localization (Lewald & Karnath, 2000; Genzel *et al.* 2016). To test whether vestibular input influences fusiform cell spatial

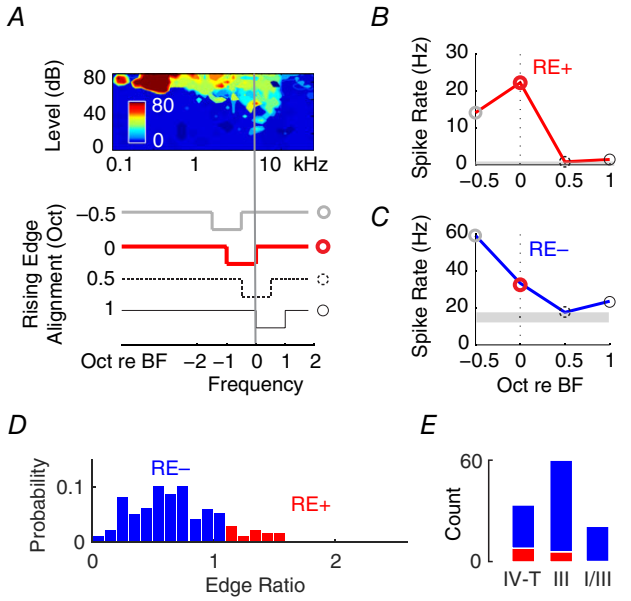

Figure 2. Spectral edge excitation in the guinea pig is rare, occurring only in some type III and IV-T fusiform cells
A, receptive field of a representative type III fusiform cell. Notches of different centre frequencies with 1 octave widths are swept across the unit's BF (vertical line) with the rising edge aligned to the notch's upper cut-off frequency. *B*, a representative example (same unit as in *A*) of rising-edge excitation (RE+; upper panel), which occurs when the 0 octave (BF-aligned) response is significantly stronger than the −0.5 octave response (off-BF). *C*, if rising-edge responses exhibit linear decreases as a function of notch upsweep (lower panel), the unit (different unit from *A* and *B*) is classified as rising-edge insensitive (RE−). *D*, edge ratio (off-BF response rate divided by BF-aligned response rate) across the population of fusiform cells, with ratios >1 indicating the RE+ response. The histogram shows a normal distribution with few RE+ response at the upper bound. *E*, numbers of RE+ and RE− response in type IV-T, III and I/III fusiform cells.

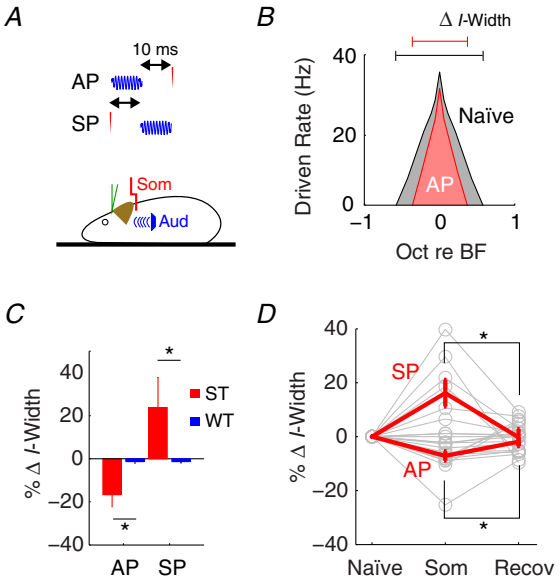

Figure 3. Somatosensory stimulation transiently alters fusiform cell sensitivity to spectral notches
A, somatosensory stimulation (transcutaneous electrical stimulation at C2; som) was paired with auditory (spectral notch) stimulation using two different timing paradigms. AP: auditory stimulus onset precedes somatosensory stimulation. SP: somatosensory stimulation precedes auditory stimulus onset. *B*, notch inhibition in a representative type IV-T fusiform cell unit under the naïve (without somatosensory) condition and during AP stimulation. *C*, changes in notch sensitivity (percentage change in *I*-width) for ST ($n = 8$) or WT ($n = 47$) units during either AP or SP stimulation. Reduced and increased *I*-width indicates improved and reduced notch detection, respectively. *D*, changes in notch sensitivity for all units ($n = 55$) during (Som: AP or SP) and immediately after (Recov) somatosensory activation. $^*P < 0.05$ (*post hoc*). Red lines indicate mean and SEM.

coding, we applied a 20° pitch tilt (Kasper *et al.* 1988) to stimulate activation of vestibular inputs to CN and compared *I*-widths of fusiform cells to the naïve condition (0° tilt) (Fig. 4*A*). Vestibular stimulation selectively affected ST units (two-way repeated-measure ANOVA, $F(1,1) = 25.1$, $P = 0.0001$ for ST *vs.* WT), by reducing their notch-detection sensitivity (increased *I*-width; $F(1,1) = 9.58$, $P = 0.0053$ for naïve *vs.* tilt; Fig. 4*B*). The effect was transient, as the increased *I*-widths were no longer observed after returning to the original 0° position (Fig. 4*C*; one-way repeated-measure ANOVA, $F(2) = 7.0$, $P = 0.003$). To control for possible alterations to fusiform cell firing rates by changing body position (Wigderson *et al.* 2016), which may obscure *I*-width calculation, we recorded rate-level functions for broad-band noise (BBN) stimulation during each condition (Fig. 4*D*) and found that tilt change did not affect fusiform cell spontaneous or evoked firing rates (two-way ANOVA, $F(17,2) = 0.26$, $P = 0.77$). The results suggest that vestibular input derived from head position plays an important role in fusiform cell spectral-notch coding.

How does altered notch-detection sensitivity in individual fusiform cells affect population coding? To assess the population response, instead of changing the notch bandwidth to quantify individual neurons, we kept the notch width constant and analysed the responses across the population of fusiform cell units with different BFs (Fig. 5). Maximal inhibition was observed for neurons with BFs within the notch bandwidth, and inhibition tapered off in neurons with BFs away from the notch centre frequency. However, the inhibitory responses for off-notch-centre neurons were strongly modulated by multisensory stimulation. Somatosensory (AP) stimulation, which sensitizes individual neuron's detection sensitivity (Fig. 3*C*), also potentiates inhibition of off-notch-centre neurons (paired *t* test, $t(38) = 4.2$, $P = 0.00014$), so that the same notch width is able to inhibit more neurons outside of the bandwidth. In contrast, somatosensory (SP) and vestibular (tilt) stimulation, which reduce notch-detection sensitivity (Figs. 3*C* and 4*B*), weaken the inhibition of neurons off-notch-centre frequency ($t(38) = -4.1$, $P = 0.00017$ for SP; $t(38) = -6.8$, $P = 5.4 \times 10^{-8}$ for Tilt). The consequence of altered inhibition off-notch-centre frequency is that the fusiform cell population becomes more (as in Tilt and SP) or less (as in AP) selective to spectral notches at a given frequency. Somatosensory and vestibular stimulation, however, do not change the best-frequency location of maximal inhibition (one-way ANOVA, $F(3) = 0.17$, $P = 0.91$), suggesting that multisensory input does not alter fusiform cell coding of notch centre frequency, but rather alters its tuning.

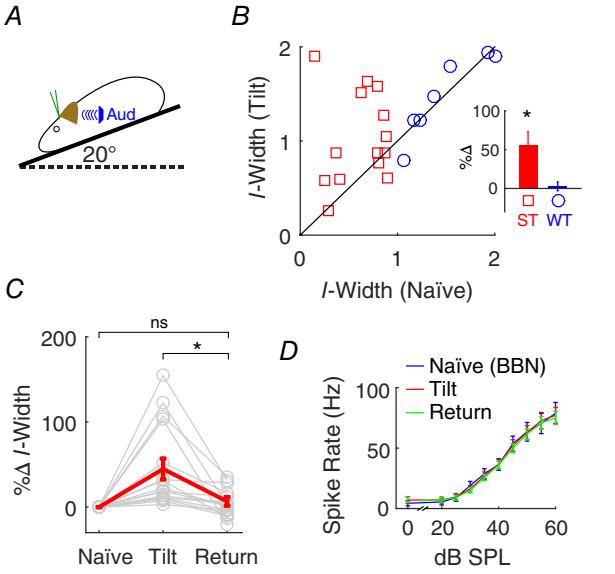

Figure 4. Vestibular stimulation transiently alters fusiform cell sensitivity to spectral notches
A, vestibular stimulation was applied during a 20° pitch tilt (left panel). *B*, fusiform cell ($n = 24$) notch responses were accessed before (naïve at 0°; horizontal axis of right panel) and during tilt stimulation (vertical axis). Data points near the diagonal line represent minimal change during tilt stimulation, while those away from the diagonal in either direction indicate increases or decreases in *I*-width during tilt stimulation. ST and WT units were distinguished by their naïve *I*-width. Inset: data plotted as percent changes in I-width. *C*, changes in *I*-width from naïve to 20° tilt, and immediately after return to the 0° (return). *D*, rate-level functions to BBN at each condition were recorded as controls. $^*P < 0.05$ (*post hoc*).

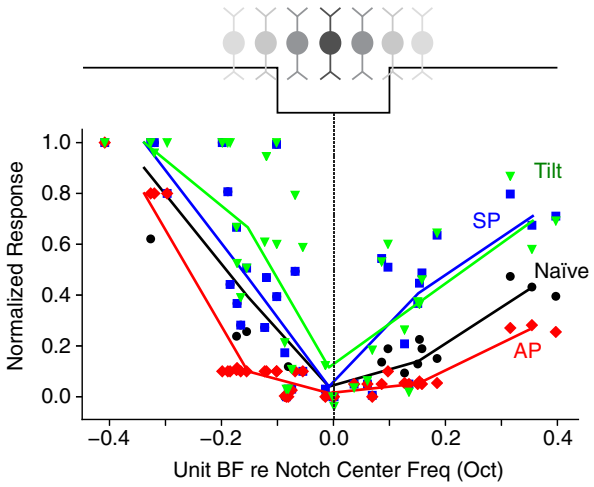

Figure 5. Differential modulation of notch inhibition sensitivity across BF affects population tuning
Black squares shows the naïve population response of 32 fusiform cells (ST response type) with different BFs to the same spectral notch stimuli (0.2 octave width, 30 dB attenuation, 50 dB SPL), normalized from 0 (spontaneous rate) to 1 (maximal firing rate driven by BBN), as a function of the neuron's BF relative to the notch centre frequency. Responses of the same neurons under somatosensory (AP, red and SP, blue) and vestibular (tilt; green) stimulation are overlaid. Lines are fitted with average values of each 0.1 octave bin.

Multisensory influence on fusiform cell spectral coding is mediated through D-stellate cells

Since multisensory inputs to fusiform cells are relayed to their apical dendrites via granule cells (Fig. 6*A*), which lack tonotopic organization (Oertel & Wu, 1989), their effects on fusiform cells are unlikely to be frequency-specific. Moreover, the fusiform cell apical dendrites are remarkably plastic (Fujino & Oertel, 2003), enabling long-term potentiation or depression by multisensory stimulation (Koehler & Shore, 2013), which was not observed here. In addition, multisensory effects were selective for fusiform cells with ST response types that receive stronger inhibition (Figs. 3*C* and 4*B*). Thus, it is more likely that multisensory inputs in the present study targeted interneurons that inhibit fusiform cells. The D-stellate cells in VCN, which have been proposed as primary regulators of spectral-notch inhibition in fusiform cells (Arnott *et al.* 2004; Lomakin & Davis, 2008), are likely candidates. Using penetrating multichannel electrodes spanning the length of DCN and VCN, we simultaneously recorded responses of fusiform cells and D-stellate cells (Fig. 6*B*). D-stellate cells showed broad tuning and On-C temporal patterns (Fig. 6*C* and *D*; Rhode, 1999; Arnott *et al.* 2004). Consistent with previous studies (Nelken & Young, 1994; Winter & Palmer,

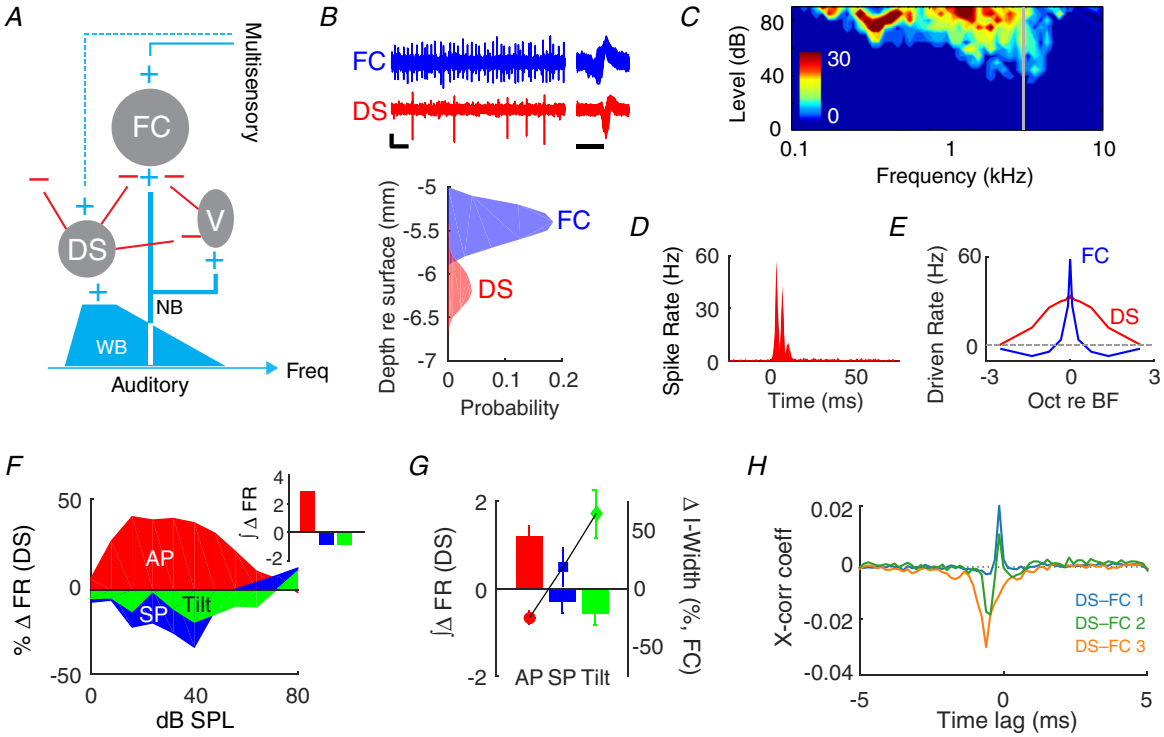

Figure 6. Multisensory responses in D-stellate cells correlate with fusiform cell spectral-notch sensitivity
A, circuit for modulating fusiform cell (FC) output. Auditory-nerve inputs innervate vertical cells (V) and basal dendrites of FCs at restricted frequencies (narrowband; NB). D-stellate cells (DS) are thought to inhibit both V and FC and can be activated by wideband (WB) auditory input. Multisensory information is transmitted to FC apical dendrites (other cell types involved in the granule cell circuit have been omitted). It is demonstrated here that multisensory information is also transmitted to DS (dashed line) to alter FC spectral-notch sensitivity. *B*, upper, representative traces of extracellular recordings from FC and DS showing good unit isolation (vertical bar: 50 μV; horizontal bar: 0.1 s). Superimposed spike waveforms are shown on the right (horizontal bar: 1 ms). Lower, depth of FC and DS units along a multiunit electrode inserted through the cerebellum into the brainstem. FCs are recorded at shallow sites in DCN (5.4 mm below the surface of the cerebellum) while DS are found at deeper sites (6.1 mm) in VCN. *C* and *D*, receptive field (*C*) and peri-stimulus time histogram (*D*) of a representative DS unit, showing broad tuning and On-C temporal response pattern. *E*, spectral-notch responses of DS and FC: FCs are strongly inhibited by notches of <1 octave width, while DS units are weakly inhibited by notches of >3 octave width. *F*, percentage change in rate-level functions for BBN for a representative DS under combined auditory and somatosensory (AP/SP) or vestibular (tilt) stimulation. Inset: sums of somatosensory- or vestibular-induced changes in DS firing rate (FR) across all sound levels. *G*, multisensory input-induced changes in cumulative FR ($\int \Delta$FR) across the DS population ($n = 54$), plotted as bars (left *y*-axis). Changes in fusiform cell spectral sensitivity (*I*-width) from Fig. 3*C* and Fig. 4*B* are plotted on the right *y*-axis. *H*, cross-correlogram of spontaneous activity for 3 different DS–FC (type III) unit pairs. 6/11 unit pairs showed both positive and negative phases (DS–FC 1, DS–FC 2), and 5/11 unit pairs showed only a prominent inhibitory phase (DS–FC 3).

1995), the cells classified as D-stellate cells were minimally affected by spectral notches due to their wide-band response areas (Fig. 6*E*).

Next, we assessed changes in D-stellate cell activity during somatosensory and vestibular stimulation (Fig. 6*F*). The rate-level functions in response to BBN increased during AP, but decreased during SP and vestibular tilt away from 0° (Fig. 6*G*; one-way ANOVA, $F(2) = 4.7$, $P = 0.011$). This bidirectional modulation of D-stellate cell firing rate inversely corresponded to the changes in fusiform cell spectral-notch sensitivity (Fig. 6*G*): increased evoked activity of D-stellate cells resulted in stronger inhibition of fusiform cells, sensitizing fusiform cell spectral-notch responses. However, since direct D-stellate cell inhibition of fusiform cells has been suggested (Arnott *et al.* 2004; Lomakin & Davis, 2008) but not yet demonstrated, we computed pairwise cross-correlations between D-stellate and fusiform cell spontaneous activity. Only type III and IV-T units were included in this analysis as type I/III units have very low spontaneous firing rates. In 11 different D-stellate-fusiform cell pairs, we observed an inhibitory (negative cross-correlation) phase in the correlogram that preceded an excitatory (positive cross-correlation) phase (Fig. 6*H*). The mean phase lags for the negative and positive phases were 1.9 ms (SD: 1.4) and 0.01 ms (SD: 0.08), respectively. The significant cross-correlations are consistent with the hypothesis that D-stellate cells provide the crucial inhibition to fusiform cells necessary for spectral-notch detection.

To determine whether multisensory neurons directly project to D-stellate cells, in separate group of guinea pigs ($n = 4$), we labelled D-stellate cells by retrograde tracer injections into the contralateral CN (Fig. 7*A*), targeting the D-stellate commissural pathway (Cant & Gaston, 1982; Doucet *et al.* 2009; Brown *et al.* 2013). In the same animals, we labelled projections from the ipsilateral cuneate nucleus with an anterograde tracer (Fig. 7*B*). Cuneate-nucleus projection terminals were observed in the magnocellular VCN in contact with dendrites (Fig. 7*C–D*) of retrogradely labelled D-stellate cells (identified by its retrograde labelling cell size typical for D-stellate cells). A higher incidence of co-labelling was found in the dorsal–lateral division of the magnocellular VCN. Taken together, the physiological and anatomical evidence presented here supports the role of D-stellate cells in CN multisensory processing of spectral notches.

Discussion

Two hypotheses prevail regarding the function of multisensory inputs to the CN. One hypothesis takes an evolutionary approach and uses electrosensory nuclei of many fish species as well as the mammalian cerebellum as analogues of the DCN circuit organization (Bell, 2002). In this model, the principal output neurons receive granule cell-relayed multisensory information, similar to that in the DCN fusiform cell circuit (Fig. 6*A*). In these structures, the circuit performs timing-based computations to extract corollary signals from the multisensory input, which

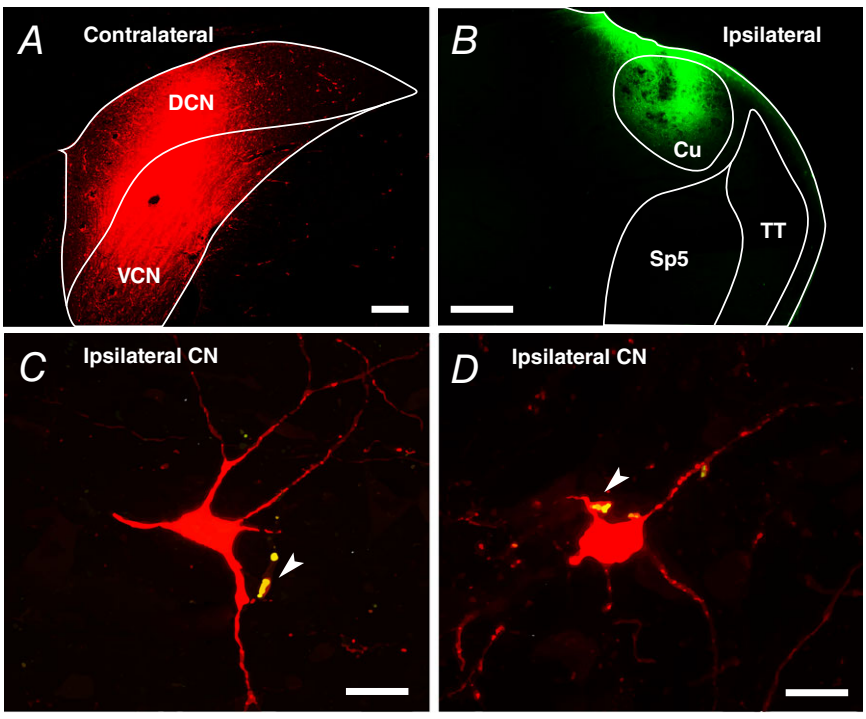

Figure 7. D-stellate cells receive somatosensory projections
A, FluoroRuby was injected into the contralateral CN (coronal section; scale bar: 0.2 mm) to label the large projection neurons (>25 μm) of the CN-commissural pathway (Doucet *et al.* 2009). *B*, FluoroEmerald was injected into the ipsilateral cuneate nucleus (Cu) (scale bar: 0.5 mm). Sp5, spinal trigeminal nucleus; TT, spinal trigeminal tract. *C* and *D*, mossy-fibre terminals from cuneate nucleus co-label (arrow on yellow) with D-stellate cell dendrite in the ipsilateral CN (scale bars: 25 μm).

cancel predicted signals such as those emitted during self-generated motion such as breathing, but amplify unpredicted, behaviourally relevant sensory inflow (Bell *et al.* 1997). Thus, in the DCN, sounds that are internally generated would produce corollary somatosensory or vestibular signals that suppress auditory-evoked responses of DCN fusiform cells (Shore, 2005). A recent study provided evidence in support of this hypothesis (Singla *et al.* 2017). However, an additional hypothesis presents the view that multisensory information encodes head and pinna orientation and actively modulates sound localization (Oertel & Young, 2004), such that changes in spectral cues induced by pinna/head movement may be 'corrected' by multisensory input. While we did not directly test this hypothesis in an actively behaving (sound-locating) animal, we showed that spectral-feature detection sensitivity was altered by somatosensory and vestibular stimulation. The present findings provide evidence in support of short-term multisensory influences on sound-localization coding, which complements the previously described, long-term multisensory influences on predicted-signal cancellation. We find here that somatosensory and vestibular input to CN can transiently alter fusiform cell detection of direction-dependent spectral notches, modulating both individual neuron's sensitivity and the population's frequency selectivity. The transient nature of the alterations, relevant for sound detection and localization, is underpinned by a novel multisensory pathway via the inhibitory D-stellate cells in VCN.

Roles of inhibition in spectral processing

Fusiform cells receive strong, narrowband inhibition from vertical cells in the deep DCN. In the cat, vertical cell-inhibition produces a central inhibitory area (CIA) in the receptive field of type IV fusiform cells (Spirou & Young, 1991). However, since spectral notches inactivate vertical cells (Nelken & Young, 1994), they cannot be responsible for spectral-notch inhibition in fusiform cells. Furthermore, type III fusiform cells (predominant in rodents; Stabler *et al.* 1996; Ma & Brenowitz, 2012), lack CIAs but can detect notches as well as type IV units in cats (Parsons *et al.* 2001; Fig. 1). Thus, another inhibitory source that produces wide-band inhibition but is not itself inactivated by spectral notches was proposed to be the key mediator of fusiform cell notch responses (Nelken & Young, 1994). The identity of the wide-band inhibitor was later suggested to be the D-stellate cell in VCN, which was shown to send diffuse projections to DCN (Arnott *et al.* 2004). The present study confirmed the interaction of D-stellate cells with fusiform cells for spectral-notch detection (Fig. 6).

While spectral-notch coding is similar across species, likely due to the concordant role of D-stellate cells, differences in vertical cell inhibition strength may contribute to the lack of rising spectral edge responses in the guinea pig (Fig. 2). In cats, spectral-edge excitation is exclusive to type IV units (Reiss and Young, 2005), and the response magnitude correlates with the size of the CIA, indicating a role for vertical cells. It was speculated that since the CIA is slightly below fusiform cell BF (Spirou & Young, 1991), significant energy in the CIA is inactivated by the BF-aligned rising edge. The present study was consistent with previous findings that type III and IV-T units, lacking CIAs, are not sensitive to rising edges (Reiss & Young, 2005; Fig. 2) – suggesting that rodents may not rely on spectral edges for spatial coding.

Multisensory integration via the inhibitory circuit

Multisensory innervation of the CN is well documented. Two major ascending somatosensory pathways, trigeminal and dorsal column systems, send collaterals to the CN (Itoh *et al.* 1987; Wright & Ryugo, 1996; Shore *et al.* 2000; Zhou & Shore, 2004; Haenggeli *et al.* 2005; Zhan *et al.* 2006). The vestibular nerve as well as secondary vestibular brainstem nuclei also project to the CN (Burian & Gstoettner, 1988; Kevetter & Perachio, 1989; Bukowska, 2002; Barker *et al.* 2012). In addition, there are significant top-down projections from regions associated with various modalities, such as collaterals from the cerebro-pontine-cerebellar pathways (Ohlrogge *et al.* 2001) and midbrain reticular formation (Zhan & Ryugo, 2007). Most of these projections terminate in the granule cell region of the CN, primarily as mossy fibre synapses on granule cells (Shore & Moore, 1998; Ryugo *et al.* 2003), which relay the inputs to fusiform cells. Some multisensory projections to the marginal regions of CN are likely processed by lesser-known cell types, such as unipolar brush or chestnut cells (Weedman *et al.* 1996; Mugnaini *et al.* 1997), whose downstream circuits remain largely unexplored (but see Borges-Merjane & Trussell, 2015). Though more sparse, multisensory inputs also terminate in the magnocellular region of the VCN (Kevetter & Perachio, 1989; Shore *et al.* 2000; Shore *et al.* 2003*a*), contacting dendrites of spherical and globular bushy cells as well as D-stellate cells (Heeringa *et al.* 2018). Somatosensory innervation of D-stellate cells may therefore be responsible for the observed inhibitory responses to somatosensory stimulation in vertical cells (Young *et al.* 1995).

A recent study showed that vestibular stimulation via body rotation elicited large, sustained increases and decreases in presumed fusiform cell spontaneous activity (Wigderson *et al.* 2016). Here, we found no evidence for such a direct vestibular effect on fusiform cells but demonstrated transient modulation of notch-detection sensitivity that corresponded to D-stellate cell inhibition (Fig. 4). D-stellate cell inhibition of fusiform cells is weak,

and the vestibular effect is only apparent through fusiform cell responses to spectral-notch stimuli. The difference in response magnitude between the two studies may be due to the different vestibular stimulation paradigms. Here we targeted the linear component via static tilt, while the study of Wigderson *et al.* targeted the angular component via body rotation. The two components are processed differently in the vestibular nuclei, which may result in different projection patterns to CN. In addition, only the saccule, conveying linear acceleration, has been shown to establish primary connections with the CN (Burian & Gstoettner, 1988; Kevetter & Perachio, 1989).

Mechanisms and implications for sound localization

Spectral notches in the head-related transfer function provide spatial information. In guinea pig as well as cat, the spectral notch occurs in the ∼10–20 kHz range (Young *et al.* 1996; Greene *et al.* 2014). However, notch-sensitive fusiform cells are present across BFs, as shown by the present study as well as previous studies in cats (Spirou & Young, 1991). We surmise that conservation of the notch-inhibition mechanism across the tonotopic axis is developmentally beneficial, as head-related transfer functions change with head/pinna size growth and vary across individuals (Anbuhl *et al.* 2017). In many auditory nuclei, neurons across the tonotopic gradient have similar characteristics, and exhibit virtually identical sound localization coding ability despite the fact that low-BF and high-BF neurons receive distinctly different sound localization cues (Griffin *et al.* 2005; Jones *et al.* 2015). Similarly, fusiform cell spectral notch sensitivity is also BF-invariant.

Fusiform cell encoding of spatial cues is enabled by D-stellate cell inhibition, which is modulated by multisensory input. Somatosensory influences on D-stellate cell responses are timing-dependent. Somatosensory preceding auditory stimulation reduced D-stellate cell firing, while auditory preceding somatosensory stimulation enhanced D-stellate cell firing (Fig. 4). Since this effect dissipated once the paired stimulation ceased, long-term plasticity was likely not involved. Instead, short-term plasticity, which is highly dependent on temporal patterns of stimulation (Fortune & Rose, 2000; Baker & Carlson, 2014), may play a key role in gating multisensory information in D-stellate cells. Bidirectional short-term plasticity is required to transmit rate information in the avian sound-localization circuit (MacLeod & Carr, 2007; MacLeod *et al.* 2007). A similar process may be involved in the D-stellate cell circuit, supported by the evidence that both fusiform and vertical cells exhibit short-term plasticity (Sedlacek & Brenowitz, 2014). Activation of multisensory input, therefore, could alter the balance of facilitation and depression, resulting in altered rate coding (Galarreta & Hestrin, 1998).

Modulation of D-stellate cell firing rate not only affects monaural processing of spectral coding in fusiform cells, as shown here, but likely also affects binaural processing since D-stellate cells send a commissural projection to the contralateral CN (Cant & Gaston, 1982; Shore *et al.* 2003*b*; Paolini *et al.* 2004; Brown *et al.* 2013). Contralateral inhibition of VCN bushy cells, T-stellate cells and DCN fusiform cells has been demonstrated (Babalian *et al.* 2002; Davis, 2005). D-stellate cell inhibition can affect both timing and intensity information of downstream processes for binaural sound localization (Grothe, 2003). Modulation of D-stellate cells may thus subserve an early mechanism for integrating multisensory information for sound localization (Lewald *et al.* 2000; Tollin *et al.* 2005).

References

Anbuhl KL, Benichoux V, Greene NT, Brown AD & Tollin DJ (2017). Development of the head, pinnae, and acoustical cues to sound location in a precocial species, the guinea pig (*Cavia porcellus*). *Hear Res* **356**, 35–50.

Arnott RH, Wallace MN, Shackleton TM & Palmer AR (2004). Onset neurones in the anteroventral cochlear nucleus project to the dorsal cochlear nucleus. *J Assoc Res Otolaryngol* **5**, 153–170.

Babalian AL, Jacomme AV, Doucet JR, Ryugo DK & Rouiller EM (2002). Commissural glycinergic inhibition of bushy and stellate cells in the anteroventral cochlear nucleus. *Neuroreport* **13**, 555–558.

Baker CA & Carlson BA (2014). Short-term depression, temporal summation, and onset inhibition shape interval tuning in midbrain neurons. *J Neurosci* **34**, 14272–14287.

Barker M, Solinski HJ, Hashimoto H, Tagoe T, Pilati N & Hamann M (2012). Acoustic overexposure increases the expression of VGLUT-2 mediated projections from the lateral vestibular nucleus to the dorsal cochlear nucleus. *PLoS One* **7**, e35955.

Bell CC (2002). Evolution of cerebellum-like structures. *Brain Behav Evol* **59**, 312–326.

Bell CC, Han VZ, Sugawara Y & Grant K (1997). Synaptic plasticity in a cerebellum-like structure depends on temporal order. *Nature* **387**, 278–281.

Blauert J (1983). Spatial hearing the psychophysics of human sound localization (MIT, Cambridge, MA), pp. 1–427.

Borges-Merjane C & Trussell LO (2015). ON and OFF unipolar brush cells transform multisensory inputs to the auditory system. *Neuron* **85**, 1029–1042.

Brown MC, Drottar M, Benson TE & Darrow K (2013). Commissural axons of the mouse cochlear nucleus. *J Comp Neurol* **521**, 1683–1696.

Bukowska D (2002). Morphological evidence for secondary vestibular afferent connections to the dorsal cochlear nucleus in the rabbit. *Cells Tissues Organs* **170**, 61–68.

Burian M & Gstoettner W (1988). Projection of primary vestibular afferent fibres to the cochlear nucleus in the guinea pig. *Neurosci Lett* **84**, 13–17.

Cant NB & Gaston KC (1982). Pathways connecting the right and left cochlear nuclei. *J Comp Neurol* **212**, 313–326.

Davis KA (2005). Contralateral effects and binaural interactions in dorsal cochlear nucleus. *J Assoc Res Otolaryngol* **6**, 280–296.

Doucet JR, Lenihan NM & May BJ (2009). Commissural neurons in the rat ventral cochlear nucleus. *J Assoc Res Otolaryngol* **10**, 269–280.

Fortune ES & Rose GJ (2000). Short-term synaptic plasticity contributes to the temporal filtering of electrosensory information. *J Neurosci* **20**, 7122–7130.

Fujino K & Oertel D (2003). Bidirectional synaptic plasticity in the cerebellum-like mammalian dorsal cochlear nucleus. *Proc Natl Acad Sci U S A* **100**, 265–270.

Galarreta M & Hestrin S (1998). Frequency-dependent synaptic depression and the balance of excitation and inhibition in the neocortex. *Nat Neurosci* **1**, 587–594.

Genzel D, Firzlaff U, Wiegrebe L & MacNeilage PR (2016). Dependence of auditory spatial updating on vestibular, proprioceptive, and efference copy signals. *J Neurophysiol* **116**, 765–775.

Greene NT, Anbuhl KL, Williams W & Tollin DJ (2014). The acoustical cues to sound location in the guinea pig (*Cavia porcellus*). *Hear Res* **316**, 1–15.

Griffin SJ, Bernstein LR, Ingham NJ & McAlpine D (2005). Neural sensitivity to interaural envelope delays in the inferior colliculus of the guinea pig. *J Neurophysiol* **93**, 3463–3478.

Grothe B (2003). New roles for synaptic inhibition in sound localization. *Nat Rev Neurosci* **4**, 540–550.

Haenggeli CA, Pongstaporn T, Doucet JR & Ryugo DK (2005). Projections from the spinal trigeminal nucleus to the cochlear nucleus in the rat. *J Comp Neurol* **484**, 191–205.

Heeringa AN, Wu C & Shore SE (2018). Multisensory integration enhances temporal coding in ventral cochlear nucleus bushy cells. *J Neurosci* **38**, 2832–2843.

Itoh K, Kamiya H, Mitani A, Yasui Y, Takada M & Mizuno N (1987). Direct projections from the dorsal column nuclei and the spinal trigeminal nuclei to the cochlear nuclei in the cat. *Brain Res* **400**, 145–150.

Jones HG, Brown AD, Koka K, Thornton JL & Tollin DJ (2015). Sound frequency-invariant neural coding of a frequency-dependent cue to sound source location. *J Neurophysiol* **114**, 531–539.

Kanold PO, Davis KA & Young ED (2011). Somatosensory context alters auditory responses in the cochlear nucleus. *J Neurophysiol* **105**, 1063–1070.

Kanold PO & Young ED (2001). Proprioceptive information from the pinna provides somatosensory input to cat dorsal cochlear nucleus. *J Neurosci* **21**, 7848–7858.

Kasper J, Schor RH & Wilson VJ (1988). Response of vestibular neurons to head rotations in vertical planes. I. Response to vestibular stimulation. *J Neurophysiol* **60**, 1753–1764.

Keating P & King AJ (2015). Sound localization in a changing world. *Curr Opin Neurobiol* **35**, 35–43.

Kevetter GA & Perachio AA (1989). Projections from the sacculus to the cochlear nuclei in the Mongolian gerbil. *Brain Behav Evol* **34**, 193–200.

Koehler SD, Pradhan S, Manis PB & Shore SE (2011). Somatosensory inputs modify auditory spike timing in dorsal cochlear nucleus principal cells. *Eur J Neurosci* **33**, 409–420.

Koehler SD & Shore SE (2013). Stimulus-timing dependent multisensory plasticity in the guinea pig dorsal cochlear nucleus. *PLoS One* **8**, e59828.

Lewald J, Dorrscheidt GJ & Ehrenstein WH (2000). Sound localization with eccentric head position. *Behav Brain Res* **108**, 105–125.

Lewald J & Karnath HO (2000). Vestibular influence on human auditory space perception. *J Neurophysiol* **84**, 1107–1111.

Lomakin O & Davis KA (2008). On the role of the wideband inhibitor in the dorsal cochlear nucleus: a computational modeling study. *J Assoc Res Otolaryngol* **9**, 506–520.

Ma WL & Brenowitz SD (2012). Single-neuron recordings from unanesthetized mouse dorsal cochlear nucleus. *J Neurophysiol* **107**, 824–835.

MacLeod KM & Carr CE (2007). Beyond timing in the auditory brainstem: intensity coding in the avian cochlear nucleus angularis. *Prog Brain Res* **165**, 123–133.

MacLeod KM, Horiuchi TK & Carr CE (2007). A role for short-term synaptic facilitation and depression in the processing of intensity information in the auditory brain stem. *J Neurophysiol* **97**, 2863–2874.

May BJ (2000). Role of the dorsal cochlear nucleus in the sound localization behavior of cats. *Hear Res* **148**, 74–87.

Mugnaini E, Dino MR & Jaarsma D (1997). The unipolar brush cells of the mammalian cerebellum and cochlear nucleus: cytology and microcircuitry. *Prog Brain Res* **114**, 131–150.

Nelken I & Young ED (1994). Two separate inhibitory mechanisms shape the responses of dorsal cochlear nucleus type IV units to narrowband and wideband stimuli. *J Neurophysiol* **71**, 2446–2462.

Oertel D & Wu SH (1989). Morphology and physiology of cells in slice preparations of the dorsal cochlear nucleus of mice. *J Comp Neurol* **283**, 228–247.

Oertel D & Young ED (2004). What's a cerebellar circuit doing in the auditory system? *Trends Neurosci* **27**, 104–110.

Ohlrogge M, Doucet JR & Ryugo DK (2001). Projections of the pontine nuclei to the cochlear nucleus in rats. *J Comp Neurol* **436**, 290–303.

Palmer AR & King AJ (1985). A monaural space map in the guinea-pig superior colliculus. *Hear Res* **17**, 267–280.

Paolini AG, Clarey JC, Needham K & Clark GM (2004). Fast inhibition alters first spike timing in auditory brainstem neurons. *J Neurophysiol* **92**, 2615–2621.

Parsons JE, Lim E & Voigt HF (2001). Type III units in the gerbil dorsal cochlear nucleus may be spectral notch detectors. *Ann Biomed Eng* **29**, 887–896.

Rees A (1996). Aligning maps of visual and auditory space. Sensory maps. *Curr Biol* **6**, 955–958.

Reiss LA & Young ED (2005). Spectral edge sensitivity in neural circuits of the dorsal cochlear nucleus. *J Neurosci* **25**, 3680–3691.

Rhode WS (1999). Vertical cell responses to sound in cat dorsal cochlear nucleus. *J Neurophysiol* **82**, 1019–1032.

Rhode WS, Smith PH & Oertel D (1983). Physiological response properties of cells labeled intracellularly with horseradish peroxidase in cat dorsal cochlear nucleus. *J Comp Neurol* **213**, 426–447.
Ryugo DK, Haenggeli CA & Doucet JR (2003). Multimodal inputs to the granule cell domain of the cochlear nucleus. *Exp Brain Res* **153**, 477–485.
Schofield BR & Cant NB (1996). Origins and targets of commissural connections between the cochlear nuclei in guinea pigs. *J Comp Neurol* **375**, 128–146.
Sedlacek M & Brenowitz SD (2014). Cell-type specific short-term plasticity at auditory nerve synapses controls feed-forward inhibition in the dorsal cochlear nucleus. *Front Neural Circuits* **8**, 78.
Shore SE (2005). Multisensory integration in the dorsal cochlear nucleus: unit responses to acoustic and trigeminal ganglion stimulation. *Eur J Neurosci* **21**, 3334–3348.
Shore SE, El Kashlan H & Lu J (2003*a*). Effects of trigeminal ganglion stimulation on unit activity of ventral cochlear nucleus neurons. *Neuroscience* **119**, 1085–1101.
Shore SE, Godfrey DA, Helfert RH, Altschuler RA & Bledsoe SC Jr (1992). Connections between the cochlear nuclei in guinea pig. *Hear Res* **62**, 16–26.
Shore SE & Moore JK (1998). Sources of input to the cochlear granule cell region in the guinea pig. *Hear Res* **116**, 33–42.
Shore SE, Sumner CJ, Bledsoe SC & Lu J (2003*b*). Effects of contralateral sound stimulation on unit activity of ventral cochlear nucleus neurons. *Exp Brain Res* **153**, 427–435.
Shore SE, Vass Z, Wys NL & Altschuler RA (2000). Trigeminal ganglion innervates the auditory brainstem. *J Comp Neurol* **419**, 271–285.
Singla S, Dempsey C, Warren R, Enikolopov AG & Sawtell NB (2017). A cerebellum-like circuit in the auditory system cancels responses to self-generated sounds. *Nat Neurosci* **20**, 943–950.
Spirou GA & Young ED (1991). Organization of dorsal cochlear nucleus type IV unit response maps and their relationship to activation by bandlimited noise. *J Neurophysiol* **66**, 1750–1768.
Stabler SE, Palmer AR & Winter IM (1996). Temporal and mean rate discharge patterns of single units in the dorsal cochlear nucleus of the anesthetized guinea pig. *J Neurophysiol* **76**, 1667–1688.
Stein BE, Stanford TR & Rowland BA (2014). Development of multisensory integration from the perspective of the individual neuron. *Nat Rev Neurosci* **15**, 520–535.
Sterbing SJ, Hartung K & Hoffmann KP (2003). Spatial tuning to virtual sounds in the inferior colliculus of the guinea pig. *J Neurophysiol* **90**, 2648–2659.
Tollin DJ, Populin LC, Moore JM, Ruhland JL & Yin TC (2005). Sound-localization performance in the cat: the effect of restraining the head. *J Neurophysiol* **93**, 1223–1234.
Weedman DL, Pongstaporn T & Ryugo DK (1996). Ultrastructural study of the granule cell domain of the cochlear nucleus in rats: mossy fiber endings and their targets. *J Comp Neurol* **369**, 345–360.
Wigderson E, Nelken I & Yarom Y (2016). Early multisensory integration of self and source motion in the auditory system. *Proc Natl Acad Sci U S A* **113**, 8308–8313.
Winter IM & Palmer AR (1995). Level dependence of cochlear nucleus onset unit responses and facilitation by second tones or broadband noise. *J Neurophysiol* **73**, 141–159.
Wright DD & Ryugo DK (1996). Mossy fiber projections from the cuneate nucleus to the cochlear nucleus in the rat. *J Comp Neurol* **365**, 159–172.
Wu C, Martel DT & Shore SE (2015). Transcutaneous induction of stimulus-timing-dependent plasticity in dorsal cochlear nucleus. *Front Syst Neurosci* **9**, 116.
Young ED & Davis KA (2002). Circuitry and function of the dorsal cochlear nucleus. In *Integrative Functions in the Mammalian Auditory Pathway*, ed. Oertel D, Fay RR & Popper AN, pp. 160–206. Springer, New York.
Young ED, Nelken I & Conley RA (1995). Somatosensory effects on neurons in dorsal cochlear nucleus. *J Neurophysiol* **73**, 743–765.
Young ED, Rice JJ & Tong SC (1996). Effects of pinna position on head-related transfer functions in the cat. *J Acoust Soc Am* **99**, 3064–3076.
Zhan X, Pongstaporn T & Ryugo DK (2006). Projections of the second cervical dorsal root ganglion to the cochlear nucleus in rats. *J Comp Neurol* **496**, 335–348.
Zhan X & Ryugo DK (2007). Projections of the lateral reticular nucleus to the cochlear nucleus in rats. *J Comp Neurol* **504**, 583–598.
Zhou J & Shore S (2004). Projections from the trigeminal nuclear complex to the cochlear nuclei: a retrograde and anterograde tracing study in the guinea pig. *J Neurosci Res* **78**, 901–907.

Additional information

Competing interests

The authors declare no competing interests.

Author contributions

C.W. and S.E.S. designed the work; C.W. acquired and analyzed data; C.W. and S.E.S. interpreted data and drafted the manuscript. Both authors approved the final version of the manuscript and agreed to be accountable for all aspects of the work in ensuring that questions related to the accuracy or integrity of any part of the work are appropriately investigated and resolved. All persons designated as authors qualify for authorship, and all who qualify for authorship are listed.

Funding

This work is funded by NIH R01-DC004825 (S.E.S.), T32-DC00011 (C.W.), P30-05188, and the University of Michigan MCubed grant.

Acknowledgments

We thank Chris Ellinger, Dwayne Valliencourt, James Wiler and David Martel for technical assistance, and Michael King for his advice on vestibular stimulation. We also thank the anonymous reviewers for constructive critiques of the manuscript.